AGU PUBLICATIONS

Geophysical Research Letters

RESEARCH LETTER
10.1002/2014GL062019

Key Points:
- Postsunset vortex develops with the onset of the prereversal enhancement
- The upper part of postsunset vortex is interrupted by turbulence
- Vortical motions in turbulent regions do not represent the postsunset vortex

Correspondence to:
W. K. Lee,
wklee@kasi.re.kr

Citation:
Lee, W. K., H. Kil, Y.-S. Kwak, and L. J. Paxton (2015), Morphology of the postsunset vortex in the equatorial ionospheric plasma drift, *Geophys. Res. Lett.*, *42*, 9–14, doi:10.1002/2014GL062019.

Received 25 SEP 2014
Accepted 5 DEC 2014
Accepted article online 9 DEC 2014
Published online 8 JAN 2015

Morphology of the postsunset vortex in the equatorial ionospheric plasma drift

Woo Kyoung Lee[1], Hyosub Kil[2], Young-Sil Kwak[1,3], and Larry J. Paxton[2]

[1]Korea Astronomy and Space Science Institute, Daejeon, South Korea, [2]Johns Hopkins University Applied Physics Laboratory, Laurel, Maryland, USA, [3]Korea University of Science and Technology, Daejeon, South Korea

Abstract The postsunset vortex in the equatorial ionosphere exhibits clockwise plasma motions after sunset in longitude (time) and altitude coordinates when the equatorial ionosphere is viewed looking northward. We describe the typical morphology of the postsunset vortex using incoherent scatter radar observations at Jicamarca in Peru during the previous solar maximum (2000–2002). A pronounced vortical plasma motion appears around 1700 LT along with the onset of the prereversal enhancement (PRE). The center of this vortex is located near an altitude of 270 km. A smaller-scale vortex also appears about 0.5 ~ 1 h later at higher altitudes. However, the morphology and occurrence time of this small vortex depend on the characteristics of the coherent backscatter region. We find that the earlier vortex is the major feature of the postsunset vortices because it is repeatable, associated with the PRE, and independent to the occurrence of the coherent backscatter region.

1. Introduction

The zonal plasma drift in the equatorial ionosphere shows a diurnal variation. Typically, the plasma drift is westward during the day and eastward at night on undisturbed days [*Fejer et al.*, 1985, 1991]. Altitudinal variation of the zonal plasma drift exists, however, and this variation is pronounced near sunset; the plasma drift is westward below the *F* region, and it is eastward within the *F* region. Theoretical studies predicted the creation of a vertical shear in the zonal plasma motion in terms of the neutral wind dynamo in the *F* region [*Farley et al.*, 1986; *Haerendel et al.*, 1992; *Rishbeth*, 1971]. This idea was supported by numerical calculations [*Eccles*, 1998; *Heelis et al.*, 1974; *Rodrigues et al.*, 2012]. The vertical shear in the zonal plasma motion, combined with the prereversal enhancement of the upward plasma drift (PRE) [*Fejer et al.*, 1979] forms a clockwise vortex in the local time (LT) (or longitude) and altitude frame when the equatorial ionosphere is viewed northward. This phenomenon is called the postsunset vortex. Supporting evidence of the postsunset vortex was provided by the observations of the vertical shear in the zonal plasma motion [*Eccles et al.*, 1999; *Kudeki et al.*, 1981; *Tsunoda et al.*, 1981; *Valenzuela et al.*, 1980] and of the vortices around coherent backscatter regions in radar observations [*Kudeki and Bhattacharyya*, 1999]. As well as providing a tool for investigating the neutral wind dynamo and the coupling of the *E* and *F* regions, this phenomenon provides a clue for the onset conditions of equatorial spread *F* [*Hysell and Kudeki*, 2004; *Hysell et al.*, 2005; *Kudeki et al.*, 2007]; the vertical shear in the zonal plasma motion associated with the postsunset vortex triggers spread *F*.

Uncertainties in the morphology of the postsunset vortex still remain because of the lack of observations. To our knowledge, *Kudeki and Bhattacharyya* [1999] (hereafter KB) is the only report that shows the full morphology of the vortical plasma motion after sunset. In their incoherent scatter radar (ISR) observations at Jicamarca Radio Observatory (JRO) (11.95°S, 76.87°W) in Peru, vortical plasma drifts develop around coherent backscatter regions. However, the vortices reported by KB are not features that can easily be identifiable in the ISR observations. Because plasma motions around the coherent backscatter region vary depending on the properties of the coherent backscatter region, it is not yet clear whether the vortical plasma motions observed around coherent backscatter regions represent the postsunset vortex predicted by theoretical studies. In addition, the vortices reported by KB were observed during a solar minimum, at a time when the PRE is typically the weakest. Although the postsunset vortex is expected to be pronounced during solar maximum because of its connection with the PRE [*Eccles et al.*, 1999], no study investigating the morphology of the postsunset vortex using the ISR data obtained during a solar maximum period has yet been reported.

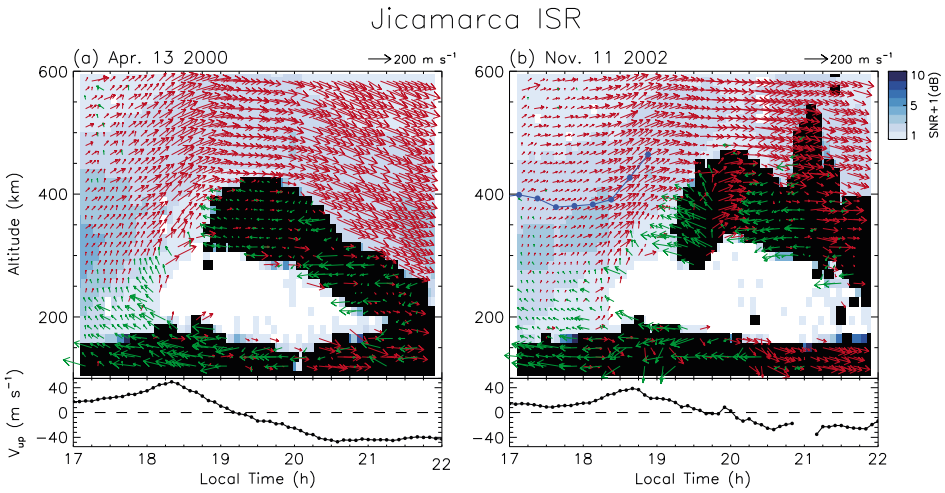

Figure 1. Typical ISR observations on (a) 13 April 2000 and (b) 11 November 2002. The color bar shows the SNR in the incoherent backscatter region. The coherent backscatter region is indicated by black. The measurements of the *F* peak height (h_mF_2) from the ionosonde at Jicamarca are shown by a blue line (Figure 1b). Green and red arrows represent westward and eastward plasma motions, respectively. The vertical velocities at the bottom of each plot are the average velocities at the altitude range of 250 and 500 km in the incoherent backscatter region.

In this study, we determine the representative morphology of the postsunset vortex from the ISR observations at JRO during solar maximum (2000–2002). The observations on two days are presented to show the variability of the plasma motions, especially in the coherent backscatter region. Then, the average drift pattern is presented to show the representative morphology of the postsunset vortex. By comparing our results with those in previous studies, we discuss the vortices in the incoherent (nonturbulent) and coherent (turbulent) backscatter regions.

2. Results

A total of 30 days of ISR data were available during the postsunset period in 2000–2002. Among those 30 days, the coherent backscatter region in the *F* region failed to appear in only three of the days in the sample period. Those three days are characterized by the occurrence of a weak PRE compared with that on the other days. The plasma motions in the incoherent backscatter region show systematic and repeatable drifts, whereas those in the coherent backscatter region are largely variable. Figure 1 presents typical ISR observations on (a) 13 April 2000 and (b) 11 November 2002. The color bar shows the signal-to-noise ratio (SNR) in the incoherent backscatter region. The coherent backscatter region is indicated by black. Green and red arrows show westward and eastward plasma motions, respectively. The measurements of the *F* peak height (h_mF_2) from the ionosonde at Jicamarca are shown by a blue line in Figure 1b. The h_mF_2 on 13 April 2000 is not shown in the figure because unrealistic values were recorded. The altitudes of peak SNR in the incoherent backscatter region are close to h_mF_2. Both peak SNR and h_mF_2 show rising of the ionosphere associated with the PRE. In both observations, the ionosphere may be divided into three regions: the incoherent backscatter region; the coherent backscatter region above an altitude of 200 km; and the coherent backscatter region below an altitude of 200 km. The ISR data are not available at the valley region located between the *E* and *F* regions. The vertical velocities at the bottom of each plot are the average velocities at the altitude range of 250 and 500 km in the incoherent backscatter region.

In Figure 1a, a vortical plasma motion is visible between 1700 and 1900 LT. At this time interval, the plasma motion is westward below an altitude of 200 km and eastward above an altitude of 300 km. The westward plasma motion weakens with increasing altitude. The upward plasma motion continues by 1900 LT. The westward and eastward plasma motions combined with the upward plasma motion comprise a clockwise vortex. The center of the vortex, even if westward plasma motions existed in the region (valley region) where data are absent, is located below an altitude of 300 km. After 1900 LT, the eastward plasma motions in the upper part of the vortex appear to be interrupted by the emergence of the coherent backscatter region. Westward and eastward plasma motions coexist in the coherent backscatter region. A vortex-like plasma

motion is also visible just before the emergence of the coherent backscatter region (near 1845 LT). This vortex can also be interpreted as the postsunset vortex, but our interpretation is that this vortex is not the main part of the postsunset vortex. Presumably, it is a remnant of the postsunset vortex developed at earlier time or associated with the emergence of the coherent backscatter region. The vortex observed in front of the coherent backscatter region is a variable feature that depends on the properties of the coherent backscatter region, whereas the vortex observed earlier is associated with the PRE and seen in most observations. For these reasons, we think that the vortex observed at earlier time is the signature feature of the postsunset vortex.

The plasma motions between 1700 and 1900 LT in Figure 1b are not as systematic as observed in Figure 1a. However, the observations of the westward and eastward plasma motions at lower and higher altitudes, respectively, are similar to those in Figure 1a. The occurrence of a weaker vortex in Figure 1b compared with that in Figure 1a may be related to the occurrence of a weaker PRE on 11 November 2002. Strong and systematic westward plasma motions exist in the coherent backscatter region. The combination of the westward plasma motions in the coherent backscatter region with eastward plasma motions above also makes vortices. If the morphology of the postsunset vortex is estimated from the observations of the shear in the zonal plasma motion without making a distinction between the incoherent and coherent backscatter regions, the vortex center appears to be located at the upper bound of the coherent backscatter region. However, those vortices, which resulted from the development of the coherent backscatter region, should be distinguished from the vortex observed before 1900 LT. Because the strong westward plasma motions in the coherent backscatter region appear at the end of the PRE, they are not interpreted as a part of the postsunset vortex.

The average pattern of plasma motions is derived using the observations when vertical backscatter plumes (plasma bubbles) are absent or minor. There were a total of 11 days that satisfied that condition. Figure 2a shows the average plasma drift pattern. The resolutions of LT and altitude are 5 min and 15 km, respectively. The average velocity in each bin was calculated with the data in both the coherent and incoherent backscatter regions. To indicate the places where the coherent backscattering occurs, the SNR map was produced with the coherent backscatter data. Because the coherent backscattering repeatedly occurs in the region indicated by the SNR map, the velocities in that region represent the plasma motions in the turbulent region. Westward and eastward plasma motions are distinguished by green and red arrows, respectively. The vertical velocities in the top panel are the observations between an altitude of 250 and 500 km in the incoherent backscatter region for the 11 days. The red line represents the average velocity. The vortical plasma motions in the incoherent backscatter region before 1900 LT are similar to those observed in Figure 1 and may represent the postsunset vortex during solar maximum. The westward and eastward plasma velocities in low and high altitudes, respectively, increase in accordance with the development of the PRE. Although uncertainties exist because of the data gap, the center of the postsunset vortex is likely located below an altitude of 300 km. The upper part of the postsunset vortex appears to be interrupted by the emergence of the coherent backscatter region. The small zonal velocities inside the coherent backscatter region, as we can see in Figure 2b, indicate the coexistence of westward and eastward plasma motions rather than stationary plasmas.

The distribution of the zonal velocity is shown in Figure 2b. Each plot presents the data within ±5 min centered at the time given on the top of each plot. The observations in the coherent and incoherent backscatter regions are distinguished by yellow and blue, respectively. At 1700 LT, a weak tendency of westward motion in low altitudes and eastward motion in high altitudes exists. As time proceeds, the increase of the westward and eastward velocities at low and high altitudes intensifies the vertical shear in the zonal drift. At 1830 LT, the transition height of the zonal velocity from westward to eastward is around 270 km. This height may represent the center of the postsunset vortex. Westward plasma motions start to appear above the transition height after 1900 LT. Those westward motions are mostly from the coherent backscatter region. Although the average zonal velocity is small in the turbulent region (see Figure 2a), the zonal velocity shows a variation in broad range. As described above, the small average velocity in the turbulent region is related to the averaging of this broad spectrum of the velocity. With the appearance of the westward motions, a new shear is formed in the region where eastward plasma motions were dominant at an earlier time. If we assess the morphology of the postsunset vortex from Figure 2b, the center of the vortex appears to continuously rise reaching an altitude of nearly 400 km at 1930 LT. However, the plasma motions in the coherent backscatter region should be distinguished from those in the incoherent backscatter region.

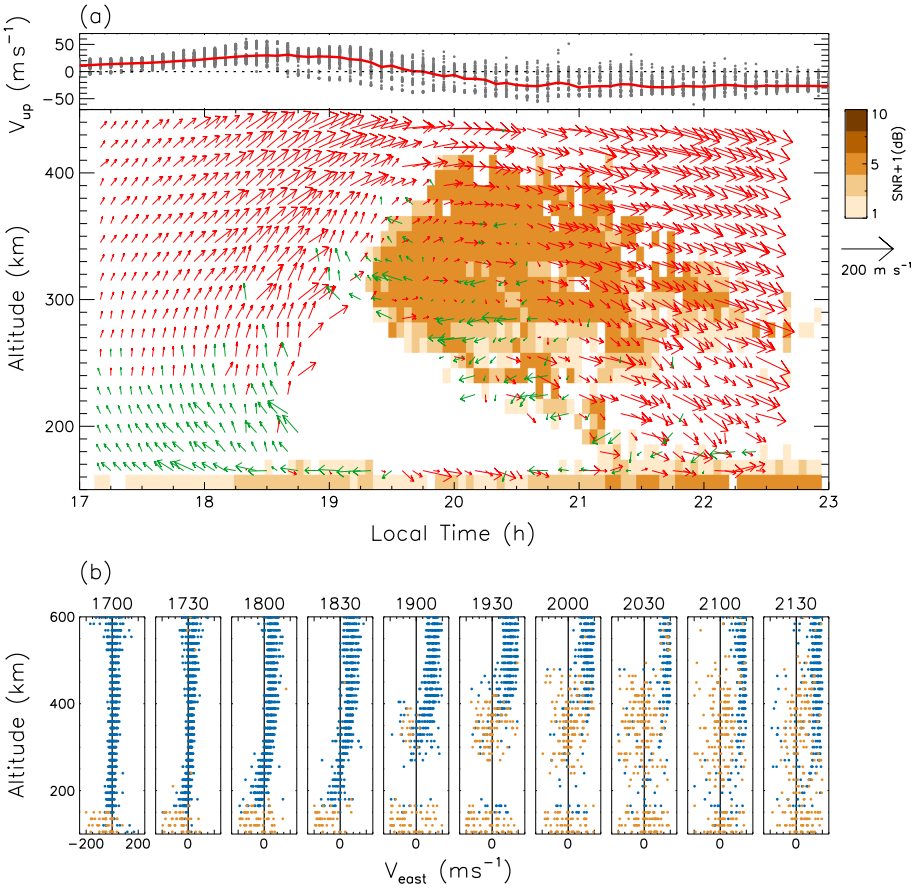

Figure 2. (a) Average plasma drift pattern over Jicamarca derived from the ISR observations of 11 days in 2000–2002 during which vertical backscatter plumes are absent or minor. The vertical velocities between an altitude of 250 and 500 km in the incoherent backscatter region and their average are shown with gray dots and a red line, respectively (top). In the velocity map (bottom), green and red arrows represent westward and eastward plasma drift, respectively. The coherent backscatter region where the number of the data in each bin is greater than 2 is indicated using the SNR. (b) Distribution of all of the measurements of the zonal velocity. Yellow and blue dots indicate the observations in the coherent and incoherent backscatter regions, respectively. Each plot presents the data within ±5 min centered at the time given on the top of each plot.

3. Discussion

The observations of the vertical shear in the zonal plasma motion are considered as evidence of the postsunset vortex, but the measurements of the shear alone provide limited information about the morphology of the postsunset vortex because a shear naturally appears in association with turbulent motion. Evidence for the existence of the vertical shear in the zonal plasma motion was provided by a chemical release experiment [*Valenzuela et al*., 1980]. The result of this experiment shows the existence of westward and eastward plasma motions below and above an altitude of 300 km, respectively, at 1900 LT. Because the ionospheric conditions at the time of the experiment are unknown, we do not know whether the shear represents the plasma motions in the nonturbulent region or turbulent region. *Kudeki et al*. [1981] and *Tsunoda et al*. [1981] identified the existence of the shear using structures in the coherent backscatter region (including vertical backscatter plumes produced by plasma bubbles). The assumption of this method is that the structures in the coherent backscatter region are good tracers of the motion of the background ionosphere. Those observations of the shear are often referred as the signature of the postsunset vortex. However, we have to consider the shear related to the development of a turbulent region. For an example, the rise of the irregularity structure inside a bubble can be associated with the growth of the bubble rather than with the upward motion of the background ionosphere. As our observations in Figure 1 show, an intense shear occurs at the boundary between the coherent and incoherent backscatter regions. This shear is

related to the development of the coherent backscatter region, and its intensity and occurrence height and time depend on the properties of the coherent backscatter region. Thus, this shear does not represent the property of the postsunset vortex. In the observation of *Kudeki et al*. [1981], the transition height of the westward and eastward plasma motions, which is interpreted as the center of the postsunset vortex, occurs as high as 450 km at 2025 LT. The authors pointed out that this height is quite high compared with that (210 km) derived from the model calculations [*Heelis et al*., 1974]. While the authors suggested the possibility of using unrealistically low *F* region height in the model calculation, the other possibility is that the transition height that they observed does not represent the center of the postsunset vortex. In our Figure 1b, the transition height is also near 450 km at 2030 LT. However, this height is the boundary of the incoherent backscatter (nonturbulent) and coherent backscatter (turbulent) regions rather than the center of the postsunset vortex.

Eccles et al. [1999] investigated the postsunset vortex using the San Marco satellite data in the nonturbulent region. However, the satellite observations were available mostly in the upper part of the postsunset vortex. The ISR observations at JRO reported by KB have been considered representative of the postsunset vortex. In their study (Plates 1 and 2), a vortical plasma motion appears near 1900 LT and its center is located near an altitude of 300 km. For both events, the coherent backscatter layer developed at the center of the vortex. Then, do those characteristics represent the postsunset vortex that the theoretical and numerical calculations predicted?

The morphology of the postsunset vortex reported by KB is somewhat different from what we observed. In our observations, a vortical plasma motion appears in accordance with the onset of the PRE (~1700 LT). We think that this vortex represents the postsunset vortex. The reasons are because this vortex is directly associated with the PRE and repeatable regardless of the development of the coherent backscatter region. Its appearance is about an hour earlier than that in KB. Although our observations were made during solar maximum when the PRE is intense, the height of the postsunset vortex center is lower than that reported by KB (The observations in KB were made during a solar minimum when the PRE is very weak.). The most significant difference between our and KB's observations is the relationship between the postsunset vortex and coherent backscatter region. In our observations, the coherent backscatter region appears in the upper part of the postsunset vortex. In the observation of KB, however, the coherent backscatter region appears near the center of the postsunset vortex.

The vortices reported by KB may be the best examples that show the vortical plasma motions around the coherent backscatter region. In most observations, the vortex around the coherent backscatter region is a weak feature. In our Figure 1a, we can identify a vortex-like plasma motion around the coherent backscatter region just before 1900 LT. Similar behavior is also visible in Figure 2a. This type of vortex may be comparable with the vortices reported by KB. If the coherent backscatter region does not develop, this type of vortex does not appear. Because the properties of this type of vortex are dependent on the properties of the coherent backscatter region, this vortex is not considered the main feature of the postsunset vortex. Radar observations show that the plasma motions in the coherent backscatter region are turbulent [e.g., *Kil et al*., 2014]. Because westward plasma motions exist in the coherent backscatter region, the development of the coherent backscatter region interrupts the eastward motions of the background plasmas. We speculate that the vortex-like plasma motion in front of the coherent backscatter region is related to this interruption.

4. Conclusions

We have investigated the morphology of the postsunset vortex in the equatorial plasma motion using the JRO ISR data acquired during solar maximum (2000–2002). A clockwise vortical plasma motion appears in accordance with the onset of the PRE. Its center is located near an altitude of 270 km. A smaller-scale vortical plasma motion also appears about 0.5 ~ 1 h later at higher altitudes. Considering the feature's repeatability and its independence of the coherent backscatter region, the former vortical plasma motion is interpreted as the signature feature of the postsunset vortex. A strong vertical shear in the zonal plasma motion exists at the upper boundary of the coherent backscatter region. However, this shear is related to the turbulent plasma motion in the coherent backscatter region rather than being associated with the postsunset vortex. This fact should be taken into account when measurements of the zonal plasma motion shear are used in the interpretation of the morphology of the postsunset vortex.

Acknowledgments
This work is supported by basic research funds from the Korea Astronomy and Space Science Institute (KASI) (2014-1-80008). H. Kil acknowledges support from National Science Foundation Aeronomy program (AGS-1237276). Y.-S. Kwak acknowledges support by a grant from the U. S. Air Force Research Laboratory, under agreement FA 2386-14-1-4004 and by the "Planetary system research for space exploration" project from KASI. The Jicamarca Radio Observatory is a facility of the Instituto Geofísico del Perú operated with support from National Science Foundation Cooperative agreement AGS-0905448 through Cornell University.

The Editor thanks two anonymous reviewers for their assistance in evaluating this paper.

References

Eccles, J. V. (1998), Modeling investigation of the evening prereversal enhancement of the zonal electric field in the equatorial ionosphere, *J. Geophys. Res.*, *103*(A11), 26,709–26,719, doi:10.1029/98JA02656.

Eccles, J. V., N. Maynard, and G. Wilson (1999), Study of the evening plasma drift vortex in the low latitude ionosphere using San Marco electric field measurements, *J. Geophys. Res.*, *104*(A12), 28,133–28,143, doi:10.1029/1999JA900373.

Farley, D. T., E. Bonelli, B. G. Fejer, and M. F. Larsen (1986), The prereversal enhancement of the zonal electric field in the equatorial ionosphere, *J. Geophys. Res.*, *91*(A12), 13,723–13.728, doi:10.1029/JA091iA12p13723.

Fejer, B. G., D. T. Farley, R. F. Woodman, and C. Calderon (1979), Dependence of equatorial *F* region vertical drifts on season and solar cycle, *J. Geophys. Res.*, *84*(A10), 5792–5796, doi:10.1029/JA084iA10p05792.

Fejer, B. G., E. Kudeki, and D. T. Farley (1985), Equatorial *F* region zonal plasma drifts, *J. Geophys. Res.*, *90*(A12), 12,249–12,255, doi:10.1029/JA090iA12p12249.

Fejer, B. G., E. R. de Paula, S. A. Gonzalez, and R. F. Woodman (1991), Average vertical and zonal *F* region plasma drifts over Jicamarca, *J. Geophys. Res.*, *96*(A8), 13,901–13,906, doi:10.1029/91JA01171.

Haerendel, G., J. V. Eccles, and S. Cakir (1992), Theory for modeling the equatorial evening ionosphere and the origin of the shear in the horizontal plasma flow, *J. Geophys. Res.*, *97*(A2), 1209–1223, doi:10.1029/91JA02226.

Heelis, R. A., P. C. Kendall, R. J. Moffet, D. W. Windle, and H. Rishbeth (1974), Electrical coupling of the *E* and *F* regions and its effect on *F* region drifts and winds, *Planet. Space Sci.*, *25*, 743–756.

Hysell, D. L., and E. Kudeki (2004), Collisional shear instability in the equatorial *F* region ionosphere, *J. Geophys. Res.*, *109*, A11301, doi:10.1029/2004JA010636.

Hysell, D. L., M. F. Larsen, C. M. Swenson, A. Barjatya, T. F. Wheeler, M. F. Sarango, R. F. Woodman, and J. L. Chau (2005), Onset conditions for equatorial spread *F* determined during EQUIS II, *Geophys. Res. Lett.*, *32*, L24104, doi:10.1029/2005GL024743.

Kil, H., W. K. Lee, Y.-S. Kwak, Y. Zhang, L. J. Paxton, and M. Milla (2014), The zonal motion of equatorial plasma bubbles relative to the background ionosphere, *J. Geophys. Res. Space Physics*, *119*, 5943–5950, doi:10.1002/2014JA019963.

Kudeki, E., and S. Bhattacharyya (1999), Postsunset vortex in equatorial *F*-region plasma drifts and implications for bottomside spread-*F*, *J. Geophys. Res.*, *104*(A12), 28,163–28,170, doi:10.1029/1998JA900111.

Kudeki, E., B. G. Fejer, D. T. Farley, and H. M. Ierkic (1981), Interferometer studies of equatorial *F* region irregularities and drifts, *Geophys. Res. Lett.*, *8*(4), 377–380, doi:10.1029/GL008i004p00377.

Kudeki, E., A. Akgiray, M. Milla, J. L. Chau, and D. L. Hysell (2007), Equatorial spread *F* initiation: Post-sunset vortex thermospheric winds, gravity waves, *J. Atmos. Sol. Terr. Phys.*, *69*, 2416–2427.

Rishbeth, H. (1971), Polarization fields produced by winds in the equatorial *F* region, *Planet. Space Sci.*, *19*, 357–369.

Rodrigues, F. S., G. Crowley, R. A. Heelis, A. Maute, and A. Reynolds (2012), On TIE-GCM simulation of the evening equatorial plasma vortex, *J. Geophys. Res.*, *117*, A05307, doi:10.1029/2011JA017369.

Tsunoda, R. T., R. C. Livingston, and C. L. Rino (1981), Evidence of a velocity shear in bulk plasma motion associated with the post-sunset rise of the equatorial *F*-layer, *Geophys. Res. Lett.*, *8*(7), 807–810, doi:10.1029/GL008i007p00807.

Valenzuela, A., G. Haerendel, E. Foppl, H. Kappler, R. F. Woodman, B. G. Fejer, and M. C. Kelley (1980), Barium cloud observations of shear flow in the postsunset equatorial *F* layer (abstract), *Eos Trans. AGU*, *61*, 315.